International Journal of Electrical, Electronics and Mechanical Controls

ISSN (Online) : 2319-7501

Volume 4 Issue 2 May 2015

Manuscript ID : ISSN23197501-V4I2M2-052015

HIGH POWER FACTOR INDUCTION HEATING SYSTEM WITH INTERLEAVED VARIABLE DUTY CYCLE

S.Ravikanth [1] V.Hanuma Naik [2]

[1]Assistant Professor, Sarojini Institute of Technology, Telaprolu, Vijayawada, Krishna Dt, A.P, India
[2]Assistant Professor, Sarojini Institute of Technology, Telaprolu, Vijayawada, Krishna Dt, A.P, India

Abstract- This project presents the analysis and design of a new ac–ac resonant converter applied to domestic induction heating. The proposed topology, based on the half-bridge series resonant inverter, uses only two diodes to rectify the mains voltage. The proposed converter can operate with zero-voltage switching during both switch-on and switch-off transitions. This modified topology and interleaved pulsing gives a nearly unity power factor. As a consequence, the converter efficiency is significantly improved. The analytical and simulation results have been verified by means of a 3600-W induction heating prototype. An efficiency study has been carried out, obtaining values higher than 96%.

Keywords-component; ac–ac resonant converter, zero-voltage switching

I. INTRODUCTION

INDUCTION heating appliance market is increasing due to its fastest heating time and efficiency. Domestic induction hobs are now becoming a standard option, especially in Asia and Europe. The principle of operation is based on the generation of a variable magnetic field by means of a planar inductor below a metallic vessel [1], [2]. The mains voltage is rectified and after that an inverter provides a medium-frequency current to feed the inductor. The usual operating frequency is higher than 20 kHz to avoid the audible range and lower than 100 kHz to reduce switching losses. The most used device is the insulated gate bipolar transistor (IGBT) because of the operating frequency range and the output power range, up to 3 kW. Nowadays, most Designs use the half-bridge series resonant topology because of its control simplicity and high efficiency [3]–[7]. In the past, several ac–ac topologies have been proposed to simplify the converter and improve the efficiency [8]–[10]. Considering the induction

Heating application, several resonant matrix converters featuring MOSFETs [11], [12], IGBTs [13], or RB-IGBTs [14], [15] have been proposed. However, the final

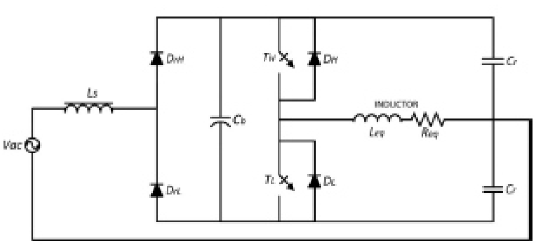

Fig. 1. Proposed ac–ac converter.

efficiency and cost are compromised due to the use of

International Journal of Electrical, Electronics and Mechanical Controls

ISSN (Online) : 2319-7501

Volume 4 Issue 2 May 2015

Manuscript ID : ISSN23197501-V4I2M2-052015

a higher number of switching devices. Other approaches, commonly used in electronic ballasts, simplify the rectifier stage in order to improve the converter performance [16]–[21]. This topology, known as half-bridge boost rectifier, reduces the switch count while keeping the same performance as more complex solutions. The aim of this paper is to propose a new topology to improve the efficiency while reducing the power device count for induction heating applications. The proposed topology is based on the series resonant half-bridge topology and requires only two rectifier diodes. The effective output voltage is doubled, as in [22], [23], allowing a significant current reduction in the switching devices. Moreover, the proposed topology can operate with zero-voltage switching conditions during turn-on for both switching devices, and also during turn-off transitions for one of them. As a consequence, the efficiency is improved while the device count is reduced. This paper is organized as follows. Section II describes the proposed topology. In Section III, a deeper analysis of the power converter is performed. Sections IV and V show the main simulation and experimental results, respectively. Finally, Section VI draws the main conclusions of this paper.

II. PROPOSED POWER CONVERTER

The proposed topology (see Fig. 1) employs two bidirectional switches *SH* and *SL* composed of a transistor *TH* or *TL* , typically an IGBT, and an ant parallel diode *DH* or *DL* , respectively. The mains voltage *v*ac is rectified by two diodes *DrH* and *DrL*, but only one of them is activated at the same time. This operation increases efficiency with regard to classical topologies based on a full-bridge diode rectifier plus a dc-link inverter. The proposed topology is a series–parallel resonant converter. The inductor–pot system is modeled as an equivalent series resistance *R*eq and inductance *L*eq, as shown.

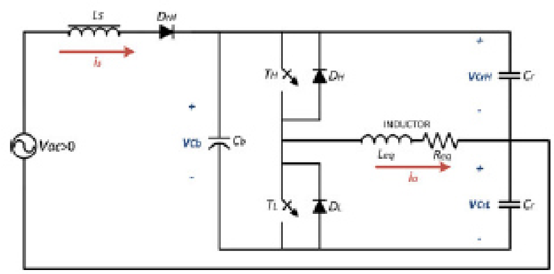

Fig. 2. Equivalent circuit during the positive mains voltage cycle.

This topology implements resonant capacitors *Cr* and may use a bus capacitor *Cb*. Due to the symmetry between positive and negative mains voltage, both resonant capacitors have the same value. An input inductor *Ls* is used to reduce the harmonic content to fulfill the electromagnetic compatibility regulations.

III. ANALYSIS

The topology presents symmetry between positive and negative ac voltage supply. Its symmetry simplifies analysis and makes possible to redraw the circuit as shown in Fig. 2. Although this topology uses different resonant configurations, parallel and series, and different resonant tanks for each of them, it is possible to use a normalized nomenclature based on series resonance

$$C_b = \alpha \cdot C_r, \quad \alpha \geq 0 \tag{1}$$

$$L_s = \beta \cdot L_{eq}, \quad \beta \geq 1 \tag{2}$$

$$\omega_0 = \frac{1}{\sqrt{L_{eq} \cdot C_r}} \tag{3}$$

$$\omega_n = \frac{\omega_{sw}}{\omega_0} \tag{4}$$

$$Z_0 = \sqrt{\frac{L_{eq}}{C_r}} \tag{5}$$

$$R_{eq} = \frac{\omega_0 \cdot L_{eq}}{Q_{eq}} = \frac{Z_0}{Q_{eq}} \tag{6}$$

Where α is the ratio between the dc-link and the resonant capacitors and β is the ratio between the input choke and the equivalent inductance of the inductor–pot system. The parameters $\{\omega_0, \omega_{sw}, \omega_n\}$ are the angular resonant frequency, the angular switching frequency, and the normalized angular switching frequency, respectively. Z_0 defines the equivalent impedance of the resonant circuit, defined by L_{eq} and C_r. Finally, Q_{eq} is the equivalent inductor–pot system quality factor at the resonant frequency. The system will be analyzed using the state-space description. Each state is completely defined by a differential equation system and the global system response is the conduction angle, θ, average response of each state (I–III):

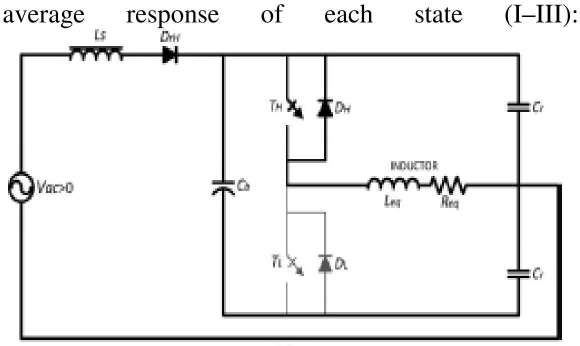

$$\dot{\mathbf{x}}(\theta) = \mathbf{A_k x}(\theta) + \mathbf{B_k} \cdot v_{ac}, \; k = \{1,2,3\}, \quad \theta = 0 \ldots 2\pi \tag{7}$$

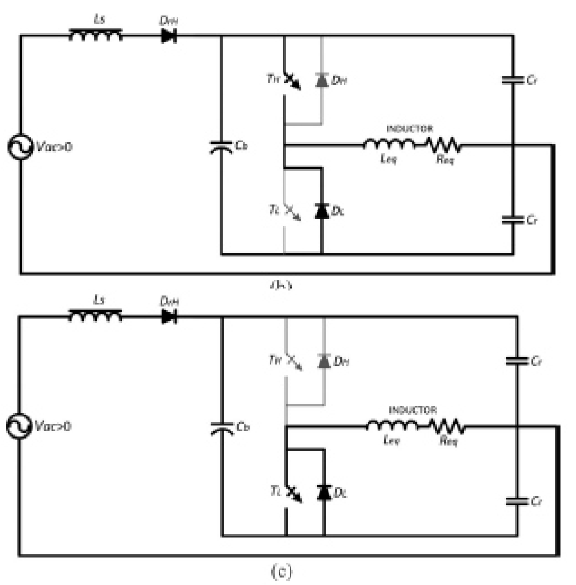

Fig. 3 Equivalent circuits. (a) State I, (b) state II, and (c) state III.

where the state variables x = [i_s, v_{Cb}, v_{CrH}, v_{CrL}, i_0]^T are the input current, the voltage across the bus capacitor C_b, the voltage across both resonant capacitors, and the current through the load, respectively. As is shown in Fig. 3, working under ZVS conditions, there are three different states. Each one has its characteristic differential equation system. Fig. 4 shows the transition conditions for each state. State I operate with the high-side switching device *SH* triggered-on and activated and the low-side switching device (*SL)* triggered-off. The parallel resonant circuit is set by an equivalent capacitor C_{eq} , obtained from C_r and C_b and expressed in (8), and the inductor electrical parameters, R_{eq} and L_{eq} . The current flowing through *SH* is the same as the one flowing through the load

$$C_{eq} = C_r \left(1 + \frac{C_b}{C_r + C_b}\right) = C_r \left(\frac{1+2\alpha}{1+\alpha}\right). \tag{8}$$

State I begins when *SL* is triggered OFF. In this moment, the anti parallel diode *DH* conducts and *SH* can be triggered ON ensuring ZVS switching-on conditions. Transitions from this state can lead either to state II or state III. If voltage across *SL* reaches zero and *DL* starts conducting, the transition condition to state II is fulfilled. On the other hand, if *SH* is switched OFF when *TH* conducts, the next state is state III. The normalized differential equations that define the dynamics of the system in this state are State II is characterized by the conduction of both switching devices, although only *SH* is triggered ON. That is, *TH* and *DL* conduct at the same time. Current through load is supplied by both devices (*TH* and *DL*), and consequently, low conduction stress for the devices is achieved. The equivalent parallel resonant circuit is set by the inductor electrical parameters in parallel with both resonant capacitors. *Cb* is short-circuited by both switching devices. This state starts when the voltage across *SL* reaches zero. At this moment, *DL* starts conducting at the same time as *TH* is triggered ON. This state finishes when *SH* is triggered OFF and the next state is state III. The main benefit results of the lower switch-off current achieved when *SH* is triggered OFF, due to the fact that the load current is supplied by both devices. In addition, *SH* achieves ZVS conditions during both switches-on and switch-off transitions, reducing consequently the switching losses. The normalized differential equati State III is defined by the

International Journal of Electrical, Electronics and Mechanical Controls

ISSN (Online) : 2319-7501

Volume 4 Issue 2 May 2015

Manuscript ID : ISSN23197501-V4I2M2-052015

conduction of *SL* while *SH* is deactivated. The equivalent resonant circuit is set by one resonant capacitor in parallel with the series connection of the *Cb* capacitor and the parallel connection of the inductor and the other one resonant capacitance. Note that when *Cb* is zero ($\alpha = 0$), the equivalent resonant circuit is a series RLC circuit composed of the inductor–pot system and one resonant capacitor. This state starts when *SH* is triggered OFF. At this moment, *DL* starts conducting and *SL* can be triggered ON achieving ZVS switch-on conditions. This state finishes when *SL* is deactivated, and the next state is state I.

IV. SIMULATION RESULTS

By using the space-state analysis presented in Section III, two operating modes can be described (see Fig. 5). Both of them achieve ZVS switch-on conditions; however, only the first operation mode can achieve the ZVS switch-off conditions for *SH* . The first operation mode uses the three states described earlier: I, II, and III. It makes possible to achieve ZVS conditions for the high-side switch in state II. The low-side switch has non- ZVS turn-off characteristic. However, turn-off current is always lower than in the high-side switch. The second operation mode only uses two states: I and III. This operation mode does not achieve ZVS conditions during switch-off, and the switching losses are, therefore, increased. This switching loss can be reduced by using snubber capacitors [25], [26]. Nowadays, the induction heating appliances' power is limited by mains maximum current and voltage. The typical maximum output power is 3600W, and the power converter prototype has been, therefore, designed to achieve 3600-W output power. Simulation parameters are *Cr* = 470 nF, and the inductor is modeled by *L*eq = 65 μH and 6.5 Ω for the series-equivalent resistor at switching frequency. The dc-link capacitor has been selected to be low enough to obtain a high power factor and a proper power control, as it is shown in this section, and it can be neglected in this analysis.

The control strategies considered to control the output power are the square wave (SW) control, based on changing the switching frequency, and the asymmetrical duty cycle control [6], [25], [27], based on changing the duty cycle of the switching devices. Next subsections detail the main simulation results.

A. SW Control Review Stage

The SW control modifies the output power by controlling the switching frequency. The switching frequency is higher than the resonant frequency to achieve switch-on ZVS, and the output power is reduced when the switching frequency is increased (see Fig. 6). As is shown in Fig. 6, the frequency range starts at 22 kHz, which is the resonant frequency determined by *L*eq and *Cr* , that ensures ZVS switching-on conditions, and can be increased to decrease the output power. However, if the switching frequency reaches 30 kHz, switching-off losses increase because ZVS switching-off conditions are not achieved. As a result, the suitable switching frequency range and, therefore, the output power range is reduced. To overcome this limitation, the asymmetric duty cycle (ADC) control strategy is proposed.

B. Asymmetrical Duty Cycle Control

The ADC control varies the output power by changing the switching device duty cycle. As is shown in Fig. 7, this control strategy delivers different output powers by changing the percent of conducting angle (θ) in which the high-side switch *SH* is activated *D*(*SH*). The low-side switch *SL* conducting angle can be calculated as follows:

$$D(S_L) = 2\pi - D(S_H) - \theta_{DT} \qquad (25)$$

where θ *DT* is the dead-time conducting angle to avoid short circuits. The variation of conducting angle is restricted by the achievement of soft-switching conditions for *SH*, ZVS for switching-off, and by the achievement of ZVS in the switching on commutation for both devices (anti parallel diode conduction at the beginning). In order to operate with switch-on ZVS conditions, the duty cycle must be higher than 30%. The upper boundary is kept to 60% to obtain a proper safety margin and balance the total amount of losses per switching device. Fig. 8 shows the power output variation achieved and the switching losses.

One of the key design aspects when designing the proposed converter to operate with the ADC control is the voltage that the switching devices must withstand. Fig. 9 shows the value of the voltage normalized to the input mains voltage as a function of the duty cycle for loads with (a) different Q_{eq} and (b)different

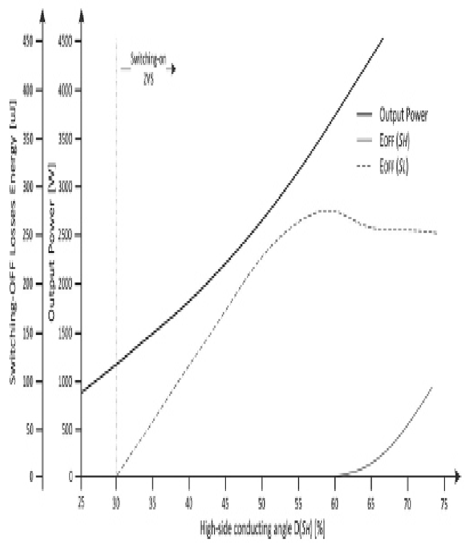

Fig. 8. Asymmetrical duty cycle control: output power and switching losses.

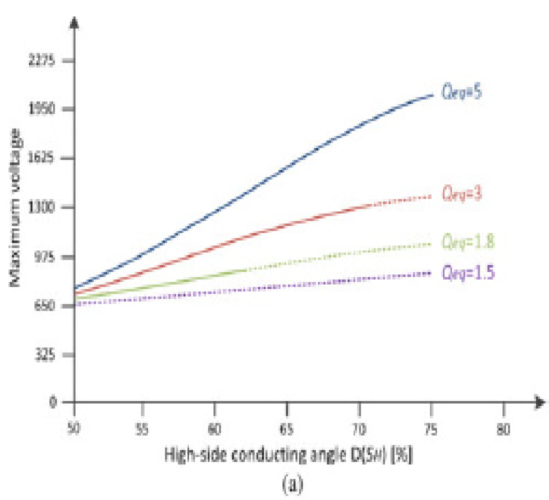

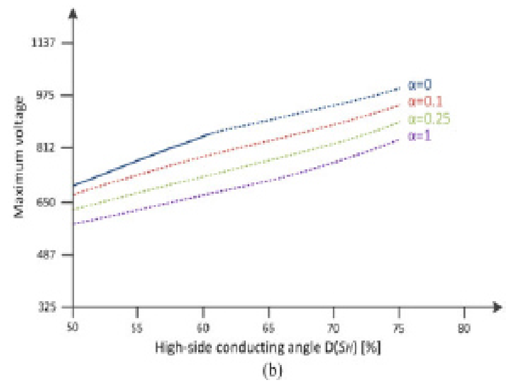

Fig. 9. Maximum voltage using 230 V rms supply voltage for different duty cycles: (a) values for different load quality factors and (b) values for different bus capacitors.

bus capacitors for the same Q_{eq} . In this figure, the optimum switching area is plotted with the solid line. As is shown in Fig. 9(a), the induction load must be carefully designed to avoid unfeasible high voltages. Besides, Fig. 9(b) shows that the bus capacitor significantly reduces the duty cycle

TABLE I
PROTOTYPE PARAMETERS

	COMPONENTS	Values
L_{eq}	Equivalent inductance	67 μH
R_{eq}	Equivalent resistance	6.5 Ω
$v_{ac,rms}$	Supply power source	230 V
C_r	Resonant capacitor	470 nF
C_b	DC-link capacitor	0 nF
L_r	Input inductance	1.4 mH
R_s	Equivalent series resistance	78 mΩ
S_H, S_L	Switching device with anti-parallel diode	IGBT FGH30RN120
D_{rH}, D_{rL}	Rectifier diodes	DESP 60-12AR

operating range, whereas the voltage in the switching device is reduced. As a conclusion, for this design the bus capacitor is removed to improve the duty cycle operating range and, consequently, the output power control, and to reduce the number of components. However, other designs with lower output power control requirements may benefit of the voltage reduction.

As a conclusion, the output power in the proposed converter can be effectively controlled by means of

International Journal of Electrical, Electronics and Mechanical Controls

ISSN (Online) : 2319-7501

Volume 4 Issue 2 May 2015

Manuscript ID : ISSN23197501-V4I2M2-052015

SW and ADC control strategies. The output power can be reduced from the maximum value at the resonant frequency, 3000W, to 1000Wwithout degrading the converter efficiency. If further reduction is required, pulse density modulation (PDM) [28] can be used to keep a high efficiency. The next section shows the main experimental results to validate the analytical and simulation results.

V. CONCLUSION

The previous papers had studied, and it is planned to implement power factor correctioin. It is planned to simulate using matlab 7.10. and hardware block diagram has been designed. The project describing a low cost solution is realized to the problem of controlling the operation of a resonant inverter designed for an induction cooker. It is very clear that operating at high frequencies in the order of 25 khz gives a better Dc voltage to the inverter circuit. More over the effficienc of the system is fine when it is operated at 25 khz. The output power is about 4.8kw. The symmetricity in the output voltage and current is obtained at high switching frequencies. The controller permits both the control of the output power level of the cooker and assures a nearly unity power factor sinusoidal current to be drawn from the mains side. The procedure is applied to the induction cooker system and the design steps and test results are presented.

REFERENCES

[1] J.Acero, J. M. Burdio, L.A. Barragan, D. Navarro, R.Alonso, J. R. Garcia, F. Monterde, P. Hernandez, S. Llorente, and I. Garde, "Domestic induction appliances," *IEEE Ind. Appl. Mag.*, vol. 16, no. 2, pp. 39–47, Mar./Apr. 2010.

[2] H. Fujita, N. Uchida, and K. Ozaki, "A new zone-control induction heating system using multiple inverter units applicable under mutual magnetic coupling conditions," *IEEE Trans. Power Electron.*, vol. 26, no. 7, pp. 2009–2017, Jul. 2010.

[3] I. Mill´an, J. M. Burd´ıo, J. Acero, O. Luc´ıa, and S. Llorente, "Series resonant inverter with selective harmonic operation applied to all-metal domestic induction heating," *IET Power Electron.*, vol. 4, pp. 587–592, May 2011.

[4] R. L. Steigerwald, "A comparison of half-bridge resonant converter topologies," *IEEE Trans. Power Electron.*, vol. 3, no. 2, pp. 174–182, Apr. 1988.

[5] H. W. Koertzen, J. D. van Wyk, and J. A. Ferreira, "Design of the halfbridge series resonant converters for induction cooking," in *Proc. IEEE Power Electron. Spec. Conf. Records*, 1995, pp. 729–735.

[6] H. Pham, H. Fujita, K. Ozaki, and N. Uchida, "Phase angle control of high-frequency resonant currents in a multiple inverter system for zonecontrol induction heating," *IEEE Trans. Power Electron.*, vol. 26, no. 11, pp. 3357–3366, Nov. 2011.

[7] W. Yunxiang, M. A. Shafi, A. M. Knight, and R. A. McMahon, "Comparison of the effects of continuous and discontinuous PWM schemes on power losses of voltage-sourced inverters for induction motor drives,"
IEEE Trans. Power Electron., vol. 26, no. 1, pp. 182–191, Jan. 2011.

First Author: S.Ravikanth**,** graduate in electrical and electronics engineering (EEE) from Prasad Institute Of Technology and Sciences, Jaggayyapet,& his M.Tech from Nalanda Institute of Engineering and Technology, Kantepudi, Sattenapalli, Guntur Dist.,A.P,India,He is working as **Assistant Professor in Dep. Of EEE at**, Sarojini Institute of Technology, Telaprolu, Vijayawada, Krishna Dt, A.P, India , Vijayawad.Affliated toJNTUK, Kakinada, A.P, India His Research Interests are **Power Systems, Power Electronics and drives, Non Conventional Energy Sources & FACTS devices.**

International Journal of Electrical, Electronics and Mechanical Controls

ISSN (Online) : 2319-7501

Volume 4 Issue 2 May 2015

Manuscript ID : ISSN23197501-V4I2M2-052015

Second Author: V.Hanuma Naik, graduate in electrical and electronics engineering (EEE) from Sri Chundi Ranganayakula engineering college, chilakaluripet,Guntur dt & his M.Tech from **National Institute of Technology Calicut Kerala, In**dia, He is working as **Assistant Professor & H**ead **O**f The **D**epartment **in Dep. Of EEE at**, Sarojini Institute of Technology, Telaprolu, Vijayawada, Krishna Dt, A.P, India, Vijayawada.Affliated to JNTUK, Kakinada, A.P, and India His Research Interests are **Power Systems, Electrical machines, Electrical measurements & FACTS devices.**